J Fluoresc (2013) 23:569–574
DOI 10.1007/s10895-013-1204-z

ORIGINAL PAPER

On the Fluorescence of Luminol in a Silver Nanoparticles Complex

Mariana Voicescu · Sorana Ionescu

Received: 27 December 2012 / Accepted: 24 February 2013 / Published online: 6 March 2013

Abstract The photophysical properties of luminol in a silver nanoparticles complex have been studied by steady-state and time resolved fluorescence spectroscopy. The effect of the serum albumin on the luminol fluorescence in the silver nanoparticles has been also investigated. It was found that the fluorescence quantum yield value of luminol in a silver nanoparticles complex is $\phi=0.00407$. The decrease of the average fluorescence lifetime value of the luminol in the silver nanoparticles complex was found to be low, $<\tau>=1.712$ ns. The luminol does not bind to the serum albumins in the presence of silver nanoparticles. The formation of a new species of luminol on silver nanoparticles is discussed. The results have influence regarding the use of luminol as an assay for bio-analytical applications.

Keywords Luminol · Silver nanoparticles · Fluorescence · Serum albumins

Introduction

Luminol (LH_2) (5-amino-2,3-dihydro-1,4-phthalazine dione) is a fluorescent substance extensively used in analytical and biochemical applications and especially in forensic medicine as tool to detect trace blood patterns [1, 2]. In aqueous medium, LH_2 presents a striking blue chemiluminescence when mixed with an oxidizing agent, fact that plays an important role in forensic applications [2]. LH_2 is intensively used as chemiluminescent probe to detect several species especially metal ions, hydrogen peroxide, nitrate, amino acids, enzyme, vitamins [3–7]. Also, the results about the effect of α, β, γ-cyclodextrin on the system that generates chemiluminescence, luminol-hydrogen peroxide in alkaline solution, pH8.5, have been reported [8].

Although the LH_2 fluorescence investigation in different solvents and solvents mixture have been reported, much less on its photo-processes in the presence of quenchers is known [9–21]. Recently, experimental and theoretical studies on the fluorescence emission of the LH_2 in several solvents have been performed [22]. It was found that hydrogen bond donation ability of the solvent represents the primary parameter controlling the excited—state behavior of LH_2 and several tautomeric forms are the principal contributors towards the LH_2 photoluminescence [22]. The biological functions of serum albumins as the major soluble protein constituents of the circulatory system are known [23, 24]. In these regards, interaction studies on the LH_2—HSA protein have been recently reported [25, 26]. Moreover, in order to be used as an efficient biomarker assay, fluorescence behavior of LH_2 in several biomimetic environments (surfactants, cyclodextrins, carrier proteins) have been performed [26]. Two LH_2 conformers present in solution, have been found and the sequestration of relatively less polar structure into the hydrophobic domain of biological media is the primary reason for LH_2 fluorescence quenching [26]. In addition, it was evidenced that the efficacy of the LH_2 fluorescence quenching, higher in micellar subdomain of cationic surfactant, depends on the nature of the head-group [26]. Moreover, detailed information regarding changes in thermodynamic parameters and binding mode of the LH_2- protein interaction have been reported [26]. In these regards, changes in the enthalpy (ΔH) and entropy (ΔS) parameters, corresponding to the binding of LH_2 in model water-soluble protein, were estimated using the fluorescence titration at different temperature. Also, the involvement of subdomain IA and IIA of bovine serum albumin

M. Voicescu (✉)
Romanian Academy, Institute of Physical Chemistry
"Ilie Murgulescu", Splaiul Independentei 202,
060021 Bucharest, Romania
e-mail: voicescu@icf.ro

S. Ionescu
Department of Physical Chemistry, University of Bucharest,
Bd Regina Elisabeta 4-12,
Bucharest 030018, Romania

(BSA) in LH_2 binding confirmed by the ligand replacement process with bilirubin, has been reported [26].

The applications of silver nanoparticles for biochemical and biomedical domains, are well known [27–33]. Recently, in these lines, experimental and simulated experiments of the serum albumins adsorbed on (non) functionalized Ag (0) nanoparticles (SNPs) have been performed [34]. It was found that the overall protein conformation upon adsorption on nanoparticle's surface is an open one which in turn results in the quenched tryptophan (Trp) fluorescence. In addition, a more hydrophilic microenvironment of the Trp residue upon protein adsorption and the fact that the surface changes did not interfere with the collisional quenching of the Trp fluorescence, have been evidenced [34].

The current paper deals with the spectrophotometric properties of LH_2 in a silver nanoparticles complex. The fluorescence intensity of luminol on addition of serum albumins and in a silver nanoparticles complex has been also measured. The results are performed in order to get more insights on LH_2 interaction with several environments and discussed with relevance to the bio-analytical applications.

Experimental

Materials Luminol (LH_2) from Fluka and DMSO from Merck, were used. BSA and HSA were purchased from Merck and used without further purification. The LH_2 concentration was 3×10^{-5}M.

The silver source, silver nitrate ($AgNO_3$, purity 99.99 %) and the reducing agent, sodium borohydride ($NaBH_4$, purity 99.8 %) were purchased from Sigma-Aldrich. SNPs were prepared according to ref. [35], by adding under vigorous stirring appropriate aliquots of 1 mM $AgNO_3$ solution to a solution containing $NaBH_4$ so that their final concentrations were 0.1 mM $AgNO_3$ and 7 mM $NaBH_4$, respectively. No capping agent was needed as the resulting nanoparticles were electrostatically stabilized [35]. To this aqueous solution, aliquots of LH_2, BSA or HSA proteins, for a final concentration of 3×10^{-5}M and 1.66 μM respectively, have been used.

Methods The absorption measurements were recorded using a Perkin Elmer, Lambda 35, UV-Vis Spectrometer at a scan rate of 480 nm/min and a spectral resolution of 1 nm.

The fluorescence emission and excitation spectra were recorded with a Jasco FP-6500 Spectrofluorometer, using 5 nm bandpasses for the excitation and the emission monochromators, the detector response of 1 s, data pitch of 1 nm, the scanning speed of 100 nm/min. The excitation wavelength was 360 nm.

The fluorescence quantum yield was determined by comparison to dilute quinine bisulfate solution in 0.1 N H_2SO_4 with 0.55 absolute quantum yield [36], using the following relationship:

$$\phi_x = (F_x A_{ref} \phi_{ref})/F_{ref} A_x$$

where F is the area under the fluorescence emission curve, for quinine bisulfate (F_{ref}) and for the studied compound (F_x) over the wavelength region 375–525 nm, A_{ref} is the absorbance for quinine bisulfate at 346 nm.

The fluorescence lifetime decays were recorded in a time-correlated single photon counting FLS920 system from Edinburgh Instruments, with laser excitation at 375 nm, a lifetime scale of 100 ns and 2048 channels. The data were fitted with a multi-exponential decay (reconvolution) and the accuracy of the fit was checked on grounds of χ^2, which was less than 1.32. Intensity-averaged lifetimes were calculated according to the equation [37]:

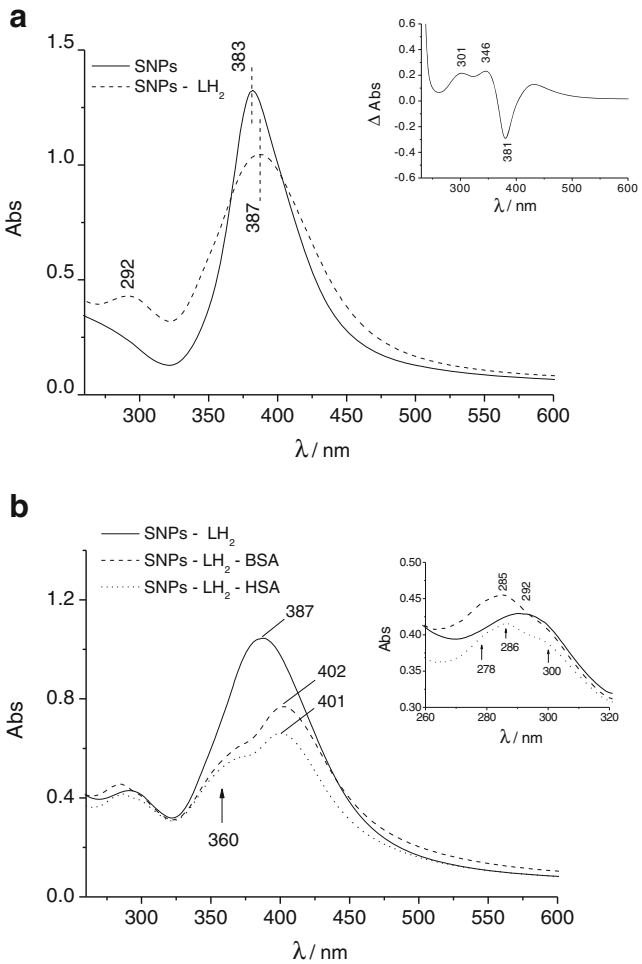

Fig. 1 UV-Vis absorption spectra of the Ag (0) nanoparticles—LH_2 complex (**a**) and Ag(0) nanoparticles—LH_2—protein complex (**b**). *Inset* shows the difference absorption spectrum, SNPs—LH_2 minus SNPs. The concentration of LH_2 is 3×10^{-5}M. The concentration of BSA and HSA proteins is 1.66 μM

$$\langle \tau \rangle = \frac{\sum_i \alpha_i \cdot \tau_i^2}{\sum_i \alpha_i \cdot \tau_i} \quad (1)$$

where α_i is the preexponential factor and τ_i the lifetime of the *i*th component. The fractional intensity of the *i*th component is defined as:

$$f_i = \frac{\alpha_i \cdot \tau_i}{\sum_i \alpha_i \cdot \tau_i} \quad (2)$$

while the fractional amplitude, interpreted as the relative population of the respective state, is:

$$a_i = \frac{\alpha_i}{\sum_i \alpha_i} \quad (3)$$

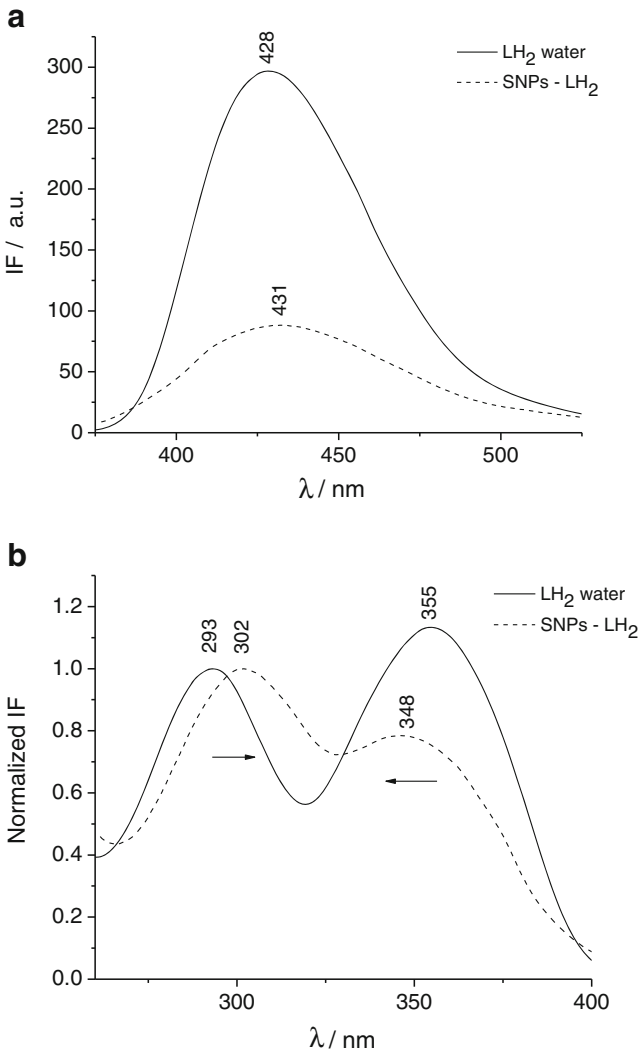

Fig. 2 Fluorescence emission (**a**) and excitation (**b**) spectra of the Ag(0) nanoparticles—LH_2 complex. The concentration of LH_2 is 3×10^{-5}M; λ_{ex}=360 nm; λ_{em}=430 nm

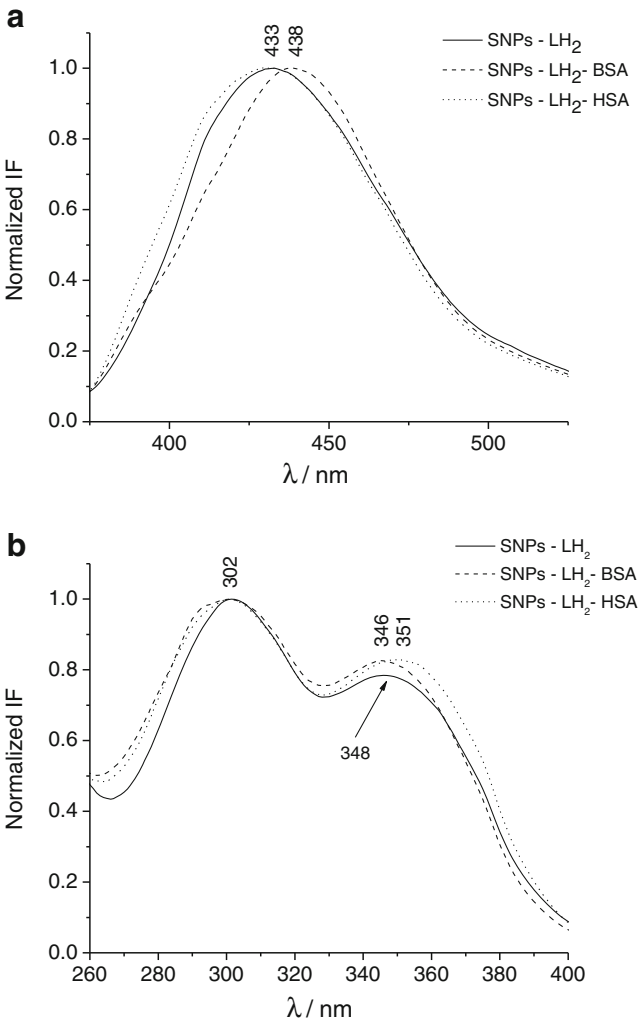

Fig. 3 Fluorescence emission (**a**) and excitation (**b**) spectra of the Ag(0) nanoparticles—LH_2—protein complex. The concentration of LH_2 is 3×10^{-5}M; The concentration of BSA and HSA proteins is 1.66 μM. λ_{ex}=360 nm; λ_{em}=430 nm

Results and Discussion

Absorption Measurements

Figure 1 presents the absorption spectra of 3×10^{-5}MLH_2 in the Ag (0) nanoparticles (SNPs)—LH_2 complex in direct comparison to the absorption spectrum of the bare SNPs (Fig. 1a). One can observe the absorption band at 383 nm, characteristics for the plasmon resonance of the SNPs, the average size of this kind of particle being of ~ 9 nm [34]. For the SNPs—LH_2 complex, two absorption bands are evidenced: the first one at 292 nm attributed to the high energy absorption band of LH_2, corresponding to the S_0 (π)→S_2 (π^*) transition. The second absorption band, 5 nm red-shifted by comparison to that of the bare SNPs, is a broad absorption band centered at 387 nm. One can thus estimate the formation

Table 1 Absorption (λ_{Abs} and ε), Emission (λ_{em} and Fluorescence Quantum Yield (ϕ_f)) and Stokes Shift ($\Delta\nu$) of the Ag(0) nanoparticles—LH_2—protein complex; λ_{ex}=360 nm

System	λ_{Abs} (nm)	ε (L $M^{-1}cm^{-1}$)	λ_{em} (nm)	$\Delta\nu$ (cm^{-1})	ϕ_f
LH_2 (aq. sol)	296/351	5700	428	4904	0.49
SNPs -LH_2	387	34800	433	5708	0.00407
SNPs -LH_2 - HSA	358/401	17400	431	5306	0.00651
SNPs -LH_2 - BSA	360/402	18700	438	6008	0.00530

of the new species, luminol anion, when LH_2 is adsorbed on the SNPs surface. *Inset* shows the difference absorption spectrum, SNPs—LH_2 minus SNPs. Two absorption bands of LH_2 are observed: the first one at 301 nm and the second one, specific to S_0 (π)→S_1 (π^*) transition, at 346 nm. The band at 381 nm corresponds to the plasmon resonance of the SNPs, the feature attributed to no changes in the size of SNPs.

When serum albumins, BSA and HSA proteins, respectively (1.66 μM) are added to the SNPs—LH_2 complex (Fig. 1b), the broad absorption band observed for SNPs—LH_2 complex is split in two absorption bands: at 360 nm attributed to the new species of luminol and, at 402 nm. The last one corresponds to the red-shift of the SNPs plasmon band, when protein accumulates at the surface [34]. It can be also observed that the shape of the absorption band in the region of 260–320 nm (Fig. 1b, *inset*) is unchanged at the addition of the serum protein to the SNPs—LH_2 complex. The absorption band around 285 nm corresponds tot the π—π^* transition of the aromatic aminoacids, Tyr and Trp [38, 39] of the serum proteins. A weak shoulder at 300 nm is visible and attributed to traces of luminol. The supposition is that no interaction between LH_2 and serum proteins takes place in the presence of SNPs.

Steady-State Fluorescence Measurements

Figure 2 shows the fluorescence emission (Fig. 2a) and excitation (Fig. 2b) spectra of LH_2 in a silver nanoparticles complex. The fluorescence intensity of the LH_2 in a SNPs complex (λ_{em}=431 nm) decreases almost three time of magnitude, becoming lower than that of the LH_2 fluorescence intensity in aqueous solution (λ_{em}=428 nm) and the wavelength emission is red shifted (5 nm) (Fig. 2a). This fact is due to the reduction of LH_2 at the SNPs surface, luminol anion being formed. Figure 2b presents the fluorescence excitation spectra of LH_2 in a silver nanoparticles complex at λ_{em}=430 nm. For a better comparison, the band I was normalized, so that significant vibrational changes in the LH_2 structure take place, one for the adsorption on SNPs surface. Comparing with the excitation spectrum of the LH_2 in aqueous solution (band II at 355 nm and band I at 293 nm, respectively) a blue-shift of 7 nm of the band II (348 nm) with a pronounced broadening as well as a 9 nm red shift (302 nm) of the high—energy band (band I) have been observed.

Figure 3 displays the normalized fluorescence emission (A) and excitation (B) spectra of the SNPs—LH_2 complex at the addition of the serum proteins. No major changes have been observed regarding the LH_2 fluorescence intensity, the only exception being a slight red shift (5 nm) at the addition of the BSA. Shoulders in the emission spectra, around 412 and 469 nm respectively, are due to the overlapping of the vibrational bands. However, slight modifications in the fluorescence emission spectra in the range of 375–410 nm, are observed (Fig. 3a). These are due to the hydrophilic regions from BSA and HSA proteins, which may be able to form the

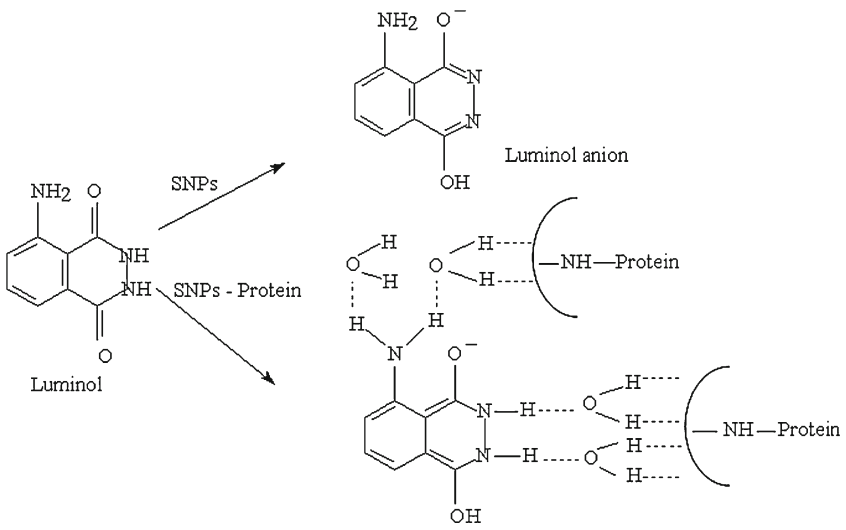

Fig. 4 The behavior of the luminol in the SNPs—proteins complex

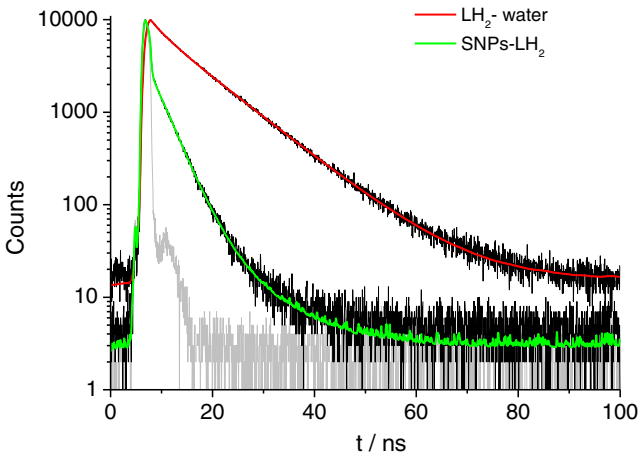

Fig. 5 Fluorescence experimental decays (*black lines*) and fit of LH_2 and Ag(0) nanoparticles—LH_2 complex. The instrument response is depicted in *gray*

intermolecular hydrogen bonds with LH_2. Also, minor changes in the normalized fluorescence excitation spectra (Fig. 3b), are evidenced. The positions of the excitation spectra are almost the same with no significant intensity changes. In addition, no wavelengths shifts were observed.

Also, no significant difference of the behavior of the SNPs—LH_2—protein complex on the excited state can be also observed in the Stokes Shift values ($\Delta\nu$=5306, for HSA and 6008 cm^{-1}, for BSA), comparatively with SNPs—LH_2 ($\Delta\nu$=5708 cm^{-1}) and with the free LH_2 ($\Delta\nu$=4904 cm^{-1}), Table 1. This is an indication that SNPs—LH_2 complex with and without serum albumins, has almost the same geometry on the excited state by comparison to that of the ground state. Moreover, the relaxation processes of LH_2 fluorescence in a SNPs complex is not influenced by serum albumins.

Overall, on the basis of these results, the behavior of the luminol in the SNPs complex as well as the position of H-bonds in the SNPs—LH_2—Protein complex are shown in the Fig. 4.

Time-Resolved Fluorescence Measurements

Figure 5 presents the intensity decays for LH_2 in water and in the presence of SNPs, with or without albumins. The reconvolution fit of the experimental decay data shows (see Table 2) that LH2 has two lifetime components of 2.56 and 10.02 ns, corresponding to the two possible species in water, neutral and anionic. The effect of the SNPs is a decrease of the decay times down to 0.10 and 3.17 ns, respectively, while further adding of either HSA or BSA very slightly increases these times. Another effect of the SNPs is the change in the fractional intensity of the two components, i.e. from 8.6 and 91.4 % to 54.7 and 49 %, meaning a shift of the acid-base equilibrium to the anion species, in accordance with the excitation spectra. As it can also be seen from the relative amplitudes, in the presence of SNPs the equilibrium is almost totally shifted towards the anion (the short component), with 97.52 % of the total amount of LH_2, while the neutral molecule amounts at 2.41 %. Adding the proteins, the intensity of the long lifetime component slightly increases to 43.4 and 45.5 % for HSA and BSA, respectively and so does the relative amplitude. A third component, of less than 4 % fractional intensity (0.06 % of the total amount of LH_2) and 9–9.4 ns is also present when adding SNPs and remains practically unchanged in the presence of proteins. It is most probably due to the non-adsorbed LH_2. One can conclude from the above experimental data that LH_2 adsorbs on the SNPs surface predominantly as anions.

Conclusions

The investigation of the fluorescence behavior of luminol in a silver nanoparticles complex reveals some special findings: i) the luminol fluorescence is quenched in the presence of silver nanoparticles; ii) luminol adsorbs on the silver nanoparticles predominantly in its anionic species; iii) the fluorescence quantum yield of luminol in the silver nanoparticles complex is slightly changed on the addition of serum albumins. The behavior is due to hydrogen bonding interaction between luminol and hydrophilic regions of serum albumins.

The fluorescence quantum yield value of luminol in a silver nanoparticles complex is lower (ϕ=0.00407) than the value of the luminol in aqueous solution (ϕ=0.49). The average fluorescence lifetime value of the luminol in the silver nano particles complex is lower (<τ>=1.712 ns) than the value of the luminol in aqueous solution (<τ>=9.366 ns).

Table 2 Fluorescence lifetimes (ns), preexponential factors, fractional amplitudes and intensities (%) of the Ag(0) nanoparticles—LH_2—protein complex

System	τ_1	α_1	a_1	f_1	τ_2	α_2	a_2	f_2	τ_3	α_3	a_3	f_3	<τ>	χ^2
LH_2 (aq. sol.)	2.56	0.012	27.27	8.61	10.02	0.032	72.73	91.39	–	–	–	–	9.366	1.130
SNPs - LH_2	0.10	0.526	97.52	54.67	3.17	0.013	2.41	41.95	9.394	3.5e−4	0.06	3.388	1.712	1.278
SNPs - LH_2-HSA	0.14	0.351	96.60	53.11	3.30	0.012	3.30	43.42	9.072	3.6e−4	0.10	3.466	1.802	1.298
SNPs - LH_2-BSA	0.16	0.311	95.58	50.74	3.25	0.014	4.30	45.52	9.269	3.9e−4	0.12	3.739	1.918	1.317

Acknowledgements This work is a part from the research project proposal, UEFISCDI, project number PN-II-RU-TE-2012-3-0055. This work has been also performed in the frame of the Romanian Academy programme of the INFRANANOCHEM Project

References

1. Kricka LJ (1995) Chemiluminescence and bioluminescence. Anal Chem 67:499R–502R
2. Yeshion TE (1991) In *Bioluminescence and Chemiluminescence: Current Status*. In: Stanley PE, Kricka LJ (eds), John Wiley: New York
3. Bowie AR, Sanders MG, Worsfold PJ (1996) Analytical applications of liquid-phase chemiluminescence reactions. A review. J Biolumin Chemilumin 11:61–90
4. Budavari S (ed) (1996) *The Merck Index*, 12th ed.; Merck & Co., Inc.: Whitehall, NJ
5. Wu Y, Zhuang Y, Liu S, He L (2008) Phenylboronic acid immunoaffinity reactor coupled with flow injection chemiluminescence for determination of α-fetoprotein. Anal Chim Acta 630:186–193
6. Zhang H, Shibata T, Krawczyk T, Kabashima T, Lu J, Lee MK, Kai M (2009) Facile detection of proteins on a solid—phase membrane by direct binding of dextran—based luminol-biotin chemiluminescent polymer. Talanta 79:700–705
7. Bi S, Zhou H, Zhang S (2009) Multilayers enzymes-coated carbon nanotubes as biolabel for ultrasensitive chemiluminescence immunoassay of cancer biomarker. Biosens Bioelectron 24:2961–2966
8. Voicescu M, Ionita G, Vasilescu M, Meghea A (2006) The effect of cyclodextrins on the luminol-hydrogen peroxide chemiluminescence. J Incl Phenom Macrocyclic Chem 54:217–219
9. Ghoneim N (1991) Solvatochromic spectroscopy of luminol in solvent mixtures. J Photochem Photobiol A: Chem 60:175–182
10. Guha D, Das R, Mitra S, Mukherjee S (1997) Fluorescence studies on Luminol in water-organic solvent mixtures. Indian J Chem 36A:307
11. Mitra S, Das R, Mukherjee S (1995) Complex formation and photophysical properties of luminol: solvent effects. J Photochem Photobiol A: Chem 87:225
12. Bhattacharjee U, Mitra S, Das R, Mukherjee S (1996) Spectroscopic studies and fluorescence quenching of luminol in aqueous medium. Indian J Chem 35A:633
13. Breslow R (1991) Hydrophobic effects on simple organic reactions in water. Acc Chem Res 24:159–164
14. Guha D, Mitra S, Das R, Mukherjee S (1999) Indian J Chem 38A:760
15. Lissi EA, Gallardo S, Sepulveda P (1992) Fluorescence quenching in cetyltrimethylammonium chloride micelles and dioctadecyldimethylammonium chloride giant vesicles. A comparison. J Colloid Interface Sci 152:104–113
16. Abuin EB, Lissi EA (1993) Quenching rate constants in aqueous solution: influence of the hydrophobic effect. J Photochem Photobiol A: Chem 71:263–267
17. Will G, Kudryashov E, Duggan E, Fitzmaurice D, Buckin V, Waghome E, Mukherjee S (1999) Excited state complex formation between 3-aminophtalhydrazide and DNA: a fluorescence quenching reaction. Spectrochim Acta Part A 55:2711–2717
18. Voicescu M, Vasilescu M, Meghea A (2000) Energy transfer from the aminophtalate dianion to fluoresceine. J Fluoresc 10:229–236
19. Voicescu M, Vasilescu M, Constantinescu T, Meghea A (2002) On the luminescence of luminol in DMSO in the presence of potassium superoxide-18 crown 6 ether and fluorescein. J Lumin 97:60–67
20. Vasilescu M, Constantinescu T, Voicescu M, Lemmetyinen H, Vuorima E (2003) Spectrophotometric study of luminol in Dimethyl sulfoxide—potassium hydroxide. J Fluoresc 13:315–322
21. Vasilescu M, Voicescu M, Lemmetyinen H (2004) Steady-state and time-resolved fluorescence of luminol in different solvent mixtures. Rev Roum Chim 49(10):841–849
22. Moyon NS, Chandra AK, Mitra S (2010) Effect of solvent hydrogen bonding on excited-state properties of luminol: a combined fluorescence and DFT study. J Phys Chem A 114:60–67
23. He XM, Carter DC (1992) Atomic structure and chemistry of human serum albumin. Nature 358:209–215
24. Olson RE, Christ DD (1996) Plasma protein binding of drugs. Ann Rep Med Chem 31:327–336
25. Moyon NS, Mitra S (2010) On the interaction of luminol with human serum albumin: nature and thermodynamics of ligand binding. Chem Phys Lett 498:178–183
26. Moyon NS, Mitra S (2011) Luminol fluorescence quenching in biomimicking environments: sequestration of fluorophore in hydrophobioc domain. J Phys Chem B 115:10163–10172
27. Salata OV (2004) Applications of nanoparticles in biology and medicine. J Nanobiotechnology Rev 23:1–6
28. Ray K, Chowdhury MH, Szmacinski H, Lakowicz JR (2008) Metal-enhanced intrinsic fluorescence of proteins on silver nanostructured surfaces towards label-free detection. J Phys Chem C 112:17957–17963
29. Szmacinski H, Ray K, Lakowicz JR (2009) Metal-enhanced fluorescence of tryptophan residues in proteins: application towards label-free bioassays. Anal Biochem 385(2):538–364
30. Levin AD, Aseichev AV, Azizova OA, Bekman EM, Vysotskii VV, Uryupina OY, Roldughin VI (2010) Modification of resonance light scattering spectra of silver nanoparticles due to their interactions with protein molecules. Colloidal J 72:23–30
31. Liu Y, Liu X, Wang X (2011) Biomimetic synthesis of gelatin polypeptide-assisted noble-metal nanoparticles and their interaction study. Nanoscale Res Lett 6(22):1–11
32. Prashant KJ, Huang X, El-Sayed IH, El-Sayed MA (2008) Noble metals on the nanoscale: optical and photothermal properties and some applications in imaging, sensing, biology and medicine. Acc Chem Res 41(12):1578–1586
33. De-Llanos R, Sanchez-Cortes S, Domingo C, Garcia-Ramos JV (2011) Surface Plasmon effects on the binding of antitumoral drug emodin to bovine serum albumin. J Phys Chem C 115:12419–12429
34. Voicescu M, Ionescu S, Angelescu DG (2012) Spectroscopic and coarse-grained simulation studies of the BSA and HAS protein adsorption on silver nanoparticles. J Nanopart Res 14:1174. doi:10.1007/s11051-012-1174-0
35. Angelescu DG, Vasilescu M, Somoghi R, Donescu D, Teodorescu VT (2010) Kinetics and optical properties of the silver nanoparticles in aqueous L64 block copolymer solutions. Colloid Surf A: Physicochem Eng Aspects 366:155–162
36. Melhuish WH (1961) J Phys Chem 65:229
37. Lakowicz JR (1983) Principles of fluorescence spectroscopy. Plenum Press, New York
38. Voicescu M, Heinrich M, Hellwig P (2009) Steady—state and time resolved fluorescence analysis of Tyrosine-Histidine model compounds. J Fluoresc 19:257–266
39. Voicescu M, El Khoury Y, Martel D, Heinrich M, Hellwig P (2009) Spectroscopic analysis of tyrosine derivatives: on the role of the Tyrosine—Histidine covalent linkage in Cytochrome c Oxidase. J Phys Chem B 113:13429–13436